Tunneling in the Loss of Hydrogen Chloride from Isopropyl Chloride Cation

Joong Chul Choe*

Department of Chemistry, University of Suwon, P.O. Box 77, Suwon 440-600, Korea

Received: February 1, 2006; In Final Form: March 3, 2006

The unimolecular dissociation of isopropyl chloride cation has been investigated using mass-analyzed ion kinetic energy spectrometry. The $C_3H_6^{\bullet+}$ ion was the only product ion in the metastable dissociation. The kinetic energy release distribution for the HCl loss was determined. Ab initio molecular orbital calculations were performed at the MP2/6-311++G(d,p) level together with single point energy calculations at the QCSID-(T)/6-311++G(2d,2p) level. The calculations show that the molecular ion rearranges to an ion−dipole complex prior to loss of HCl via a transition state containing a four-membered ring. The rearrangement involves H atom transfer. On the basis of the potential energy surface obtained for the loss of HCl and Cl$^{\bullet}$, the rate constants were calculated by transition-state statistical theories with considering tunneling effect. From the calculated result, it is proposed that the observed HCl loss would occur via tunneling through the barrier for isomerization to the ion−dipole complex, $CH_3CHCH_2^{\bullet+}\cdots HCl$.

1. Introduction

Tunneling is one of the most interesting phenomena to arise from quantum mechanics. In chemical reactions occurring through a barrier, especially involving H atom transfer, tunneling can be observed. Experimental evidence for the tunneling effect in ionic dissociations has been reported.[1−7] The techniques used for recent observations include photoelectron photoion coincidence (PEPICO)[3,4] and tandem mass spectrometry.[6,7] Tunneling-corrected transition-state rate constants can be evaluated using an algorithm reported by Miller.[8] A potential energy surface (PES) constructed by quantum chemical molecular orbital calculations is useful for theoretical prediction of the tunneling effect. It has been reported that tunneling plays important roles in dissociations of some aliphatic halide cations. In the PEPICO studies by Baer and co-workers it has been demonstrated that loss of HX (X = Cl or Br) from ethyl chloride[3] and isobutyl bromide[4] cations can occur by tunneling. Recently, we have proposed that loss of X$^{\bullet}$ from propargyl chloride[7] and bromide[6] cations can occur by tunneling using tandem mass spectrometry.

According to recent studies on the dissociation of isopropyl chloride cation ($CH_3CHClCH_3^{\bullet+}$) using PEPICO[9] and photoionization (PI)[10] methods, loss of Cl$^{\bullet}$ dominates near the threshold. The PI result shows that the Cl$^{\bullet}$ loss dominates at energies up to 1 eV above the threshold. The HCl loss, not mentioned in those studies, appears in the electron ionization (EI) mass spectrum[11−13] of isopropyl chloride. It is expected that the HCl loss occurs by rearrangement and the Cl$^{\bullet}$ loss by direct bond cleavage. In general, dissociation by rearrangement is less favorable at high energies in competition with direct bond cleavage considering an entropic factor. This suggests that the HCl loss observed in EI would occur from the molecular ions having low internal energies, seemingly inconsistent with no detection of it in the PEPICO and PI studies.

In this work, we try to elucidate the dissociation mechanism for loss of HCl from isopropyl chloride cation. The unimolecular dissociation of isopropyl chloride cation has been investigated using mass-analyzed ion kinetic energy spectrometry (MIKES),[14] a technique of tandem mass spectrometry. The kinetic energy release distribution (KERD) for the HCl loss has been determined. The PES for the HCl and Cl$^{\bullet}$ loss has been explored by ab initio molecular orbital calculations. The rate constants have been calculated using the tunneling-corrected Rice-Ramsperger-Kassel-Marcus (RRKM) theory[8,15] and phase space theory (PST)[15,16] to understand the dissociation dynamics.

2. Methods

Experimental. A double-focusing mass spectrometer with reverse geometry (VG ZAB-E) was used. Isopropyl chloride purchased from Aldrich was used without further purification and was ionized by 70-eV electron ionization. Ion source temperature was maintained at 150 °C, and ions generated were accelerated to 8 keV. MIKES was used to observe the unimolecular dissociation of metastable isopropyl chloride cation, that is, the metastable dissociation. The molecular ion was selected by the magnetic sector, and the translational kinetic energy of a product ion generated in the second field-free region of the instrument was analyzed by the electric sector. The time between the molecular ion formation and its unimolecular dissociation, namely the lifetime of the metastable ion, can be estimated from its flight time from the ion source to the dissociation region. This is 23 μs for isopropyl chloride cation accelerated to 8 keV, evaluated by assuming that the dissociation occurs at the focal point of the second field-free region. To improve the quality of a MIKE spectrum, signal averaging was carried out for repetitive scans.

Computational. Molecular orbital calculations were performed with the Gaussian 98 suite of programs.[17] Geometry optimizations for the molecular ion, intermediate, and fragments were carried out at the unrestricted MP2[18] level using the 6-311++G(d,p) basis set. A transition-state geometry connecting the molecular ion with the intermediate to lose HCl was searched and checked by calculating the intrinsic reaction coordinate (IRC) at the same level. The harmonic vibrational frequencies and the zero-point vibrational energies (ZPVEs) for the optimized structures were calculated at the same level and

* Corresponding author phone: +82-31-220-2150; fax: +82-31-222-9385; e-mail: jcchoe@suwon.ac.kr.

10.1021/jp060673p CCC: $33.50
Published on Web 03/29/2006

scaled down by 0.9496 and 0.9748, respectively.[19] Single point energies were calculated at the QCISD(T)[20]/6-311++G(2d,-2p) level with geometries optimized at the MP2/6-311++G-(d,p) level.

The RRKM expression[15] was used to calculate the rate-energy dependences

$$k(E) = \frac{\sigma N^{\neq}(E - E_0)}{\rho(E)} \quad (1)$$

where E is the reactant internal energy, E_0 is the critical energy of the reaction, $N^{\neq}$ is the sum of states of the transition state, ρ is the density of states of the reactant, and σ is the reaction path degeneracy. When a reaction was subject to quantum mechanical tunneling, $N^{\neq}(E)$ was replaced by $N^{\neq}_{\text{tunnel}}(E)$ as proposed by Miller[8,15]

$$N^{\neq}_{\text{tunnel}}(E - E_0) = \int_{-E_0}^{E-E_0} \kappa(\epsilon)\rho^{\neq}(E - E_0 - \epsilon)d\epsilon \quad (2)$$

where ϵ is the translational energy in the one-dimensional reaction coordinate, $\rho^{\neq}$ is the density of states of the transition state, and κ is the tunneling probability calculated by treating the barrier along the reaction coordinate as the Eckart potential.[21] $N^{\neq}$, ρ, and $\rho^{\neq}$ were evaluated by direct count of vibrational states using the Beyer−Swinehart algorithm.[15,22]

The PST[15,16] rate calculation for the $Cl^{\bullet}$ loss was carried out using the formalism modified by Chesnavich and Bowers.[16,23,24] The model assumes an orbiting transition state (OTS) located at the centrifugal barrier and that orbital rotational energy at this transition state is converted into relative translational energy of the products. The OTS/PST rate expression is given by

$$k(E,J) = \frac{S\int_{E^*_{\text{tr}}}^{E-E_0} \rho_{\text{v}}(E - E_0 - E_{\text{tr}})\Gamma_{\text{ro}}(E_{\text{tr}},J)\text{d}E_{\text{tr}}}{h\rho_{\text{v}}'(E,J)} \quad (3)$$

where J is the total angular momentum, S is the symmetry number ratio of reactant to products, ρ_{v} and ρ_{v}' are the product and reactant vibrational state densities, respectively, E_{tr} is the product translational energy sum, E^*_{tr} is the minium value of E_{tr}, and Γ_{ro} is the product sum of rotational-orbital states with rotational orbital energy less than or equal to E_{tr}. $k(E)$ was obtained by averaging eq 3 with the rotational thermal distribution.

3. Results and Discussion

In the metastable dissociation of isopropyl chloride ion, $C_3H_6^{\bullet+}$ was the predominant product ion. The MIKE spectrum for the metastable dissociation is shown in Figure 1a. The $C_3H_6^{\bullet+}$ peak looks dish-topped, and a weak sharp peak is superimposed onto the dish-topped peak. The weak $C_3H_5^+$ and $C_3H_7^+$ peaks were detected also. When He collision gas was introduced in the collision cell located in the second-field free region, the intensities of the $C_3H_5^+$ and $C_3H_7^+$ peaks increased with the collision gas pressure. The shape and intensity of the $C_3H_6^{\bullet+}$ peak, however, was not affected by the collision pressure. This indicates that only the $C_3H_6^{\bullet+}$ peak is due to the genuine metastable dissociation, while the other weak peaks are due to collision-induced dissociation by the residual gas. The continuum background on the high-energy side of the $C_3H_6^{\bullet+}$ peak is due to the dissociation occurring inside the electric sector. The low-energy half of the peak was used to evaluate KERD according to the well-established method.[25] The

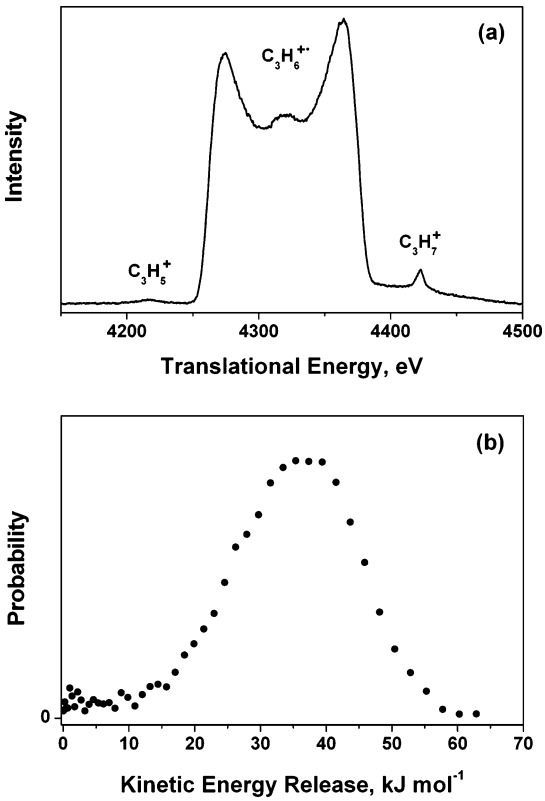

Figure 1. (a) The MIKE spectrum of the metastable dissociation of isopropyl chloride cation generated by electron ionization. (b) The KERD for the HCl loss from metastable isopropyl chloride cation, evaluated for the $C_3H_6^{\bullet+}$ profile in (a).

KERD for the HCl loss obtained by analyzing the profile in Figure 1a is shown in Figure 1b.

It seems that observation of the metastable dissociation occurring after the time delay of ~20 μs is not compatible with the previous results. According to the PEPICO study by Baer et al.,[9] the dissociation rate constant of the molecular ion is larger than could be determined by the technique (10^7 s^{-1} or larger) at the appearance of $C_3H_7^+$. In a study by Hudson et al.,[10] the dissociation rate constant was estimated as ~10^{10} s^{-1} by RRKM calculations at the energy just above the threshold. One possibility of the occurrence of metastable dissociation is involvement of a long-lived excited electronic state (so-called isolated state) dissociating slowly. To our knowledge, however, any evidence for such a possibility has not been reported in dissociations of alkyl halide cations including the molecular ion. The other possibility, more probable, is the metastable dissociation by tunneling through a barrier to lose HCl, occurring below the dissociation limit to the $Cl^{\bullet}$ loss. Similarly, it has been suggested that the HX loss detected in PEPICO experiments occurs by tunneling from ethyl chloride and isobutyl bromide cations.[3,4] To investigate the second possibility, the PES for the dissociation was constructed by quantum chemical molecular orbital calculations.

According to the present MP2/6-311++G(d,p) calculations, the molecular ion isomerizes to an ion−dipole complex (CH_3-$CHCH_2^{\bullet+}\cdots HCl$) prior to loss of HCl. Their optimized structures are shown in Figure 2 (see Table 1 for energetic data). One of the C−C bonds is elongated upon ionization of isopropyl chloride. The C1−C2 bond (1.700 Å) is longer than the C2−C3 bond (1.506 Å) (see Figure 2 for numbering of atoms). The H1 atom of the C1 methyl group moves toward the Cl atom to form the ion−dipole complex via a transition state containing a four-membered ring (see Figure 2). The ion−dipole complex

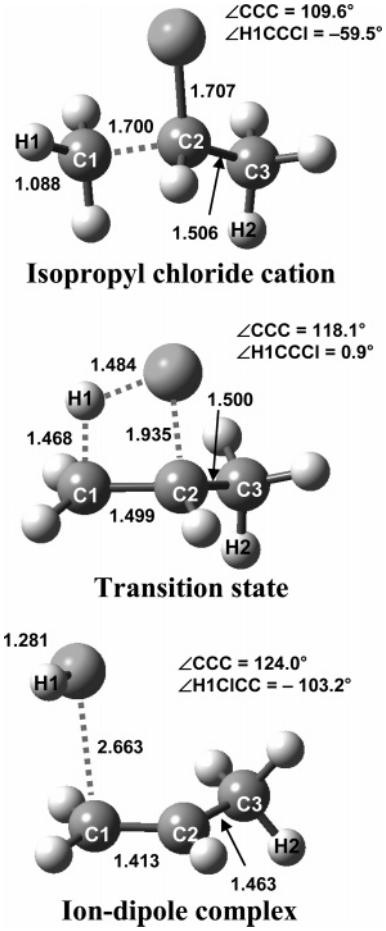

Figure 2. Geometrical structures of the molecular ion, transition state, and ion−dipole complex for loss of HCl optimized at the MP2/6-311++G(d,p) level. The numbers are the bond lengths in Å.

TABLE 1: Calculated and Experimental Relative Energies (kJ mol^{-1}) of Relevant Species

species	MP2[a]	QCISD(T)[b]	exp $\Delta_f H^\circ_{0K}$
$CH_3CHClCH_3^{\bullet+}$	0.00	0.00	0
transition state[c]	55.40	45.42	
$CH_3CHCH_2^{\bullet+}\cdots HCl$	−42.96	−63.94	
$CH_3CHCH_2^{\bullet+}$ + HCl	−16.51	−36.40	−30[d]
c-$C_3H_6^{\bullet+}$ + HCl	25.32	13.34	21[d]
$CH_3CHCH_3^+$ + Cl$^\bullet$	33.38	16.18	26,[e] 29[f]

[a] Calculated at the MP2/6-311++G(d,p)//MP2/6-311++G(d,p) level. The ZPVE calculated and scaled by 0.9748 is included. [b] Calculated at the QCISD(T)/6-311++G(2d,2p)//MP2/6-311++G(d,p) level. The ZPVE calculated at the MP2/6-311++G(d,p) level and scaled by 0.9748 is included. [c] Connecting $CH_3CHClCH_3^{\bullet+}$ with $CH_3CHCH_2^{\bullet+}\cdots HCl$. [d] Reference 26. The $\Delta_f H^\circ_{0K}$ values for $CH_3CHClCH_3^{\bullet+}$ (909 kJ mol^{-1}), and $CH_3CHCH_2^{\bullet+}$ (971 kJ mol^{-1}) were converted from the reported 298 K values by adding the respective average thermal energies, derived using calculated ZPVEs scaled by 0.9748. [e] PI result in ref 10. [f] PEPICO result in ref 9.

can dissociate to propylene ion ($CH_3CHCH_2^{\bullet+}$) and HCl by cleavage of the weak C1−Cl bond. The structures of the CH_3-$CHCH_2$ and HCl moieties of the ion−dipole complex are very similar to the $CH_3CHCH_2^{\bullet+}$ and HCl products, respectively. On the other hand, the ion−dipole complex can undergo further isomerizations to produce cyclopropane ion (c-$C_3H_6^{\bullet+}$). This pathway is initialized by migration of the H2 atom to the C2 atom together with migration of HCl to the C3 atom. The remaining steps are very similar to those for the production of c-$C_3H_6^{\bullet+}$ and H_2O from $CH_2CH_2CH_2OH_2^{\bullet+}$, which has been reported in a recent study on the dissociation of 1-propanol

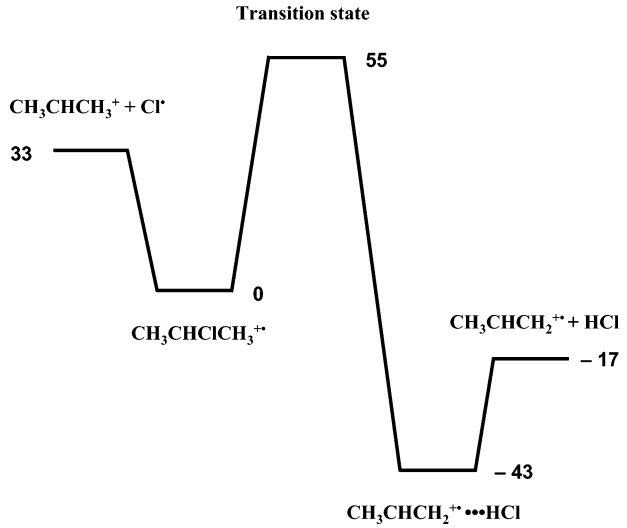

Figure 3. Potential energy diagram for loss of HCl and Cl$^\bullet$ from isopropyl chloride cation derived from the MP2/6-311++G(d,p)//MP2/6-311++G(d,p) calculations. The numbers are the relative energies in kJ mol^{-1}.

cation.[27] The endoergicity as well as the energy barrier for the production of c-$C_3H_6^{\bullet+}$ + HCl from the ion−dipole complex, however, is much higher than that for $CH_3CHCH_2^{\bullet+}$ + HCl (See Table 1). Therefore, the production of c-$C_3H_6^{\bullet+}$ would be much less favorable in competition with that of $CH_3CHCH_2^{\bullet+}$, of which details will not be described here.

The calculated relative energies of the products are compared with experimental ones in Table 1. The calculated relative energies of $CH_3CHCH_3^+$ + Cl$^\bullet$ and c-$C_3H_6^{\bullet+}$ + HCl are close to experimental ones, and that of $CH_3CHCH_2^{\bullet+}$ + HCl is higher than the experimental energy by 13 kJ mol^{-1}. The result of single point energy calculations at the QCISD(T)/6-311++G-(2d,2p) level is not better than the MP2 result in comparing with the experimental data. Therefore, we will report the RRKM model calculation result carried out by using the MP2 energetic data.

As shown in the PES of Figure 3, the barrier for the HCl loss is higher than that for the Cl$^\bullet$ loss. As mentioned above, the Cl$^\bullet$ loss is faster than 10^7 s^{-1} at the energy just above the threshold according to the PEPICO experiment.[9] Apparently, the HCl loss can be hardly observed above the isomerization barrier because it is much less favorable entropically as well than the Cl$^\bullet$ loss. It can occur, however, by tunneling through the barrier because the rearrangement involves migration of H atom. We carried out RRKM model calculations for the isomerization rate constant, k_{isom},with considering the tunneling effect. For calculations of the tunneling probability (κ) by assuming the Eckart barrier, the forward and backward barrier heights of 55.40 and 98.36 kJ mol^{-1} (the MP2 result), respectively, were used (see eq 7.67 on page 265 in ref 15 for κ). The imaginary frequency (1164 cm^{-1}) scaled by 0.9496 was used, which expresses the curvature of the barrier. The tunneling probability calculated is shown in Figure 4 as a function of the internal energy. The other vibrational frequencies used in the RRKM rate calculations are listed in Table 2. The calculated rate-energy dependence is shown in Figure 5. In the dissociation to $CH_3CHCH_2^{\bullet+}$ + HCl, the isomerization to the ion−dipole complex is the rate-determining step, since the followed dissociation occurs much faster. For example, at the energy of 33 kJ mol^{-1}, the calculated k_{isom} is 3.5×10^4 s^{-1}. According to a rough RRKM estimation, the rate constant of the dissociation $CH_3CHCH_2^{\bullet+}\cdots HCl \rightarrow CH_3CHCH_2^{\bullet+}$ + HCl is larger than 10^{10}

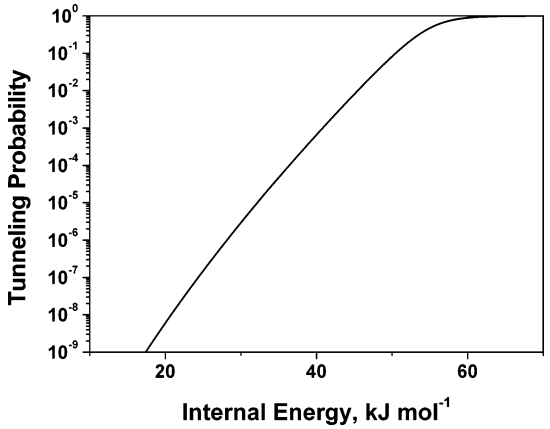

Figure 4. Tunneling probability for the isomerization ($CH_3CHClCH_3^{\bullet+}$ → $CH_3CHCH_2^{\bullet+}\cdots HCl$) barrier calculated by assuming as the Eckart barrier.

TABLE 2: Parameters Used in the RRKM and PST Calculations

species	vibrational frequencies,[a] cm^{-1}
$CH_3CHClCH_3^{\bullet+}$	192,[d] 221,[d] 242,[d] 313,[d] 375,[d] 686, 829, 872, 890, 926, 1023, 1074, 1217, 1289, 1345, 1350, 1395, 1410, 1413, 2358, 2923, 2927, 2977, 3013, 3038, 3093, 3102
transition state[b]	1164*i*, 250, 260, 273, 372, 440, 499, 770, 843, 906, 918, 958,918, 958, 1099, 1126, 1196, 1306, 1359, 1394, 1410, 1428, 1494, 2920, 2994, 3007, 3032, 3044, 3116
$CH_3CHCH_3^+$	174, 231, 404, 564, 571, 901, 932, 1032, 1164, 1204, 1253, 1258, 1300, 1309, 1392, 1432, 1488, 2741, 2758, 2975, 2976, 3021, 3070, 3070
$CD_3CDClCD_3^{\bullet+}$	138,[e] 174,[e] 209,[e] 268,[e] 331,[e] 585, 631, 650, 699, 712, 817, 904, 954, 987, 1005, 1012, 1020, 1035, 1124, 2020, 2100, 2141, 2190, 2233, 2253, 2308, 2375
transition state[c]	869*i*, 182, 186, 241, 311, 413, 438, 556, 667, 700, 712, 763 857, 913, 962, 1005, 1010, 1023, 1086, 1102, 1237, 2100, 2168, 2226, 2239, 2257, 2326

species	rotational constants,[f] cm^{-1}			polarizability,[g] 10^{-24} cm^3
$CH_3CHClCH_3^{\bullet+}$	0.257	0.162	0.110	
$CH_3CHCH_3^+$	1.36	0.288	0.260	
$Cl^{\bullet}$				2.18

[a] Calculated at the MP2/6-311++G(d,p) level and scaled by 0.9496. *i* denotes the imaginary frequency. [b] Connecting $CH_3CHClCH_3^{\bullet+}$ with $CH_3CHCH_2^{\bullet+}\cdots HCl$. [c] Connecting $CD_3CDClCD_3^{\bullet+}$ with $CD_3CDCD_2^{\bullet+}\cdots DCl$. [d] These were replaced by 50, 70, 120, 140, 206 for the transition state in the RRKM calculation for the $Cl^{\bullet}$ loss with $\Delta S^{\ddagger}_{1000K} = 29$ J mol^{-1} K^{-1}. The 686 cm^{-1} mode was taken as the reaction coordinate. [e] These were replaced by 18, 60, 105, 180, 260 for the transition state in the RRKM calculation for the $Cl^{\bullet}$ loss with $\Delta S^{\ddagger}_{1000K} = 29$ J mol^{-1} K^{-1}. The 817 cm^{-1} mode was taken as the reaction coordinate. [f] Calculated at the MP2/6-311++G(d,p) level. [g] Reference 28.

s^{-1} at the same energy. This means also that if the isomerization occurs in the ion source, all of the formed ion−dipole complexes would dissociate prior to exit from the ion source. As shown in Figure 5, the isomerization and hence the HCl loss can occur below the critical energy with considerable rates.

To predict whether the HCl loss can be observed experimentally, the rate constants should be compared with those for the other competitive channel, the $Cl^{\bullet}$ loss. We could not locate a transition state connecting the molecular ion and $CH_3CHCH_3^+ + Cl^{\bullet}$, indicating that the dissociation occurs via a "loose" transition state. First, we estimated the rate constant, k_{-Cl}, using

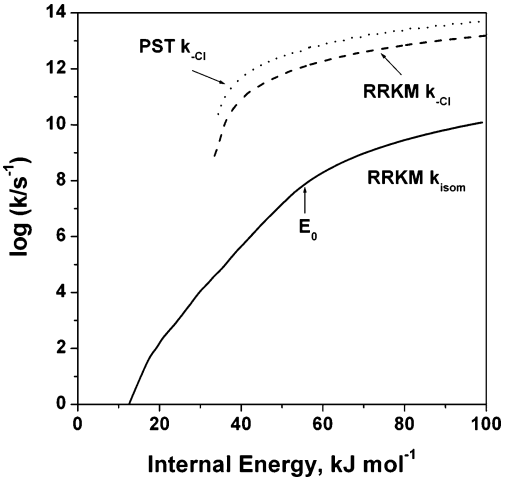

Figure 5. Theoretical rate-energy dependences for the isomerization ($CH_3CHClCH_3^{\bullet+}$ → $CH_3CHCH_2^{\bullet+}\cdots HCl$, k_{isom}) and the $Cl^{\bullet}$ loss ($CH_3CHClCH_3^{\bullet+}$ → $CH_3CHCH_2^{\bullet+}$ + HCl, k_{-Cl}). The critical energy for the isomerization is denoted as the vertical arrow.

the PST formalism of eq 3 by assuming an OTS. The molecular parameters used in the calculation are listed in Table 2. The resultant rate-energy dependence is shown in Figure 5. The rate constants are much larger than those for the $Cl^{\bullet}$ loss. However, generally the phase space rate constants are considered upper limits in the statistical approximation since a totally loose transition state is assumed.[16,24] Namely, the OTS/PST calculation could overestimate the rate constants. Therefore, we estimated k_{-Cl} roughly by RRKM theory using a criterion of activation entropy. It is well-known that RRKM rate constants depend on the activation entropy, not on the individual vibrational frequencies. Usually, the transition-state vibrational frequencies are adjusted using the activation entropy at 600 or 1000 K.[15,29,30] Most of the 1000 K activation entropy ($\Delta S^{\ddagger}_{1000K}$) values reported in ref 29 and in subsequent work for reactions occurring via a loose transition state are in the range of 13−46 J mol^{-1} K^{-1} (3.0−11 eu). Therefore, the lower five vibrational frequencies of the molecular ion were adjusted for $\Delta S^{\ddagger}_{1000K}$ to become 29 J mol^{-1} K^{-1}, the middle of the range, and used for the loose transition state (see Table 2 for the parameters used). Recently, Hudson et al.[10] performed an RRKM model calculation for the same dissociation. They have located a transition state with an extended C2−Cl bond distance (3.930 Å calculated at the B3LYP/6-311G(d,p) level) and used it in the RRKM calculation, even though it does not connect the molecular ion with $CH_3CHCH_3^+$ and $Cl^{\bullet}$ according to their IRC calculations. The $\Delta S^{\ddagger}_{1000K}$ evaluated with the vibrational frequencies reported by the investigators is 22 J mol^{-1} K^{-1}, close to the value used here. The critical energy, $E_0(-Cl)$, of 33.38 kJ mol^{-1} obtained by MP2 calculations was used. The calculated rate-energy dependence is shown in Figure 5. The rate constants are still much larger than those for the HCl loss, even though smaller than the PST rate constants.

At 0.1 kJ mol^{-1} above $E_0(-Cl)$, the calculated RRKM rate constant for the $Cl^{\bullet}$ loss is 8×10^8 s^{-1}, agrees with the PEPICO result ($>10^7$ s^{-1}). At the same energy, that for the HCl loss by tunneling is 4×10^4 s^{-1}. At higher energies also, the rates for the HCl loss are much slower than for the $Cl^{\bullet}$ loss by 4 orders of magnitude as shown in Figure 5. This indicates that the HCl loss cannot compete with the $Cl^{\bullet}$ loss above $E_0(-Cl)$. This prediction agrees well with the PEPICO and PI results, no detection of $C_3H_6^{\bullet+}$ at the energies above appearance of $C_3H_7^+$. Below $E_0(-Cl)$, however, only the HCl loss can occur with the rate constant less than 4×10^4 s^{-1}. From the calculated rate-

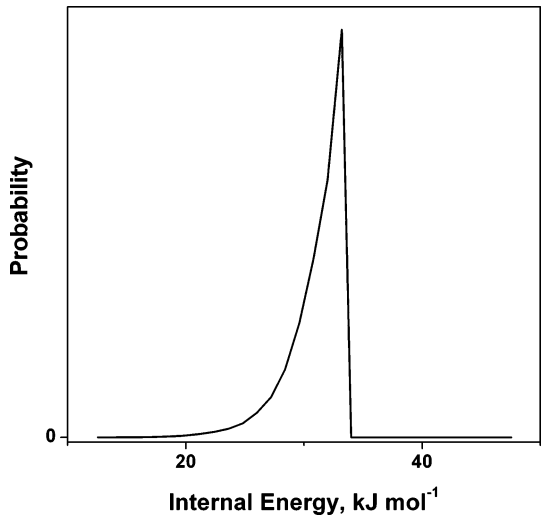

Figure 6. Internal energy distribution of isopropyl chloride cations undergoing the metastable dissociation.

energy dependences, we can predict which reaction(s) would be detected in the metastable dissociation. From the random lifetime assumption,[14,16] the probability that a dissociating ion of energy E will have lifetime τ is given by

$$P_\tau(E) = k_{tot}(E)e^{-k_{tot}(E)\tau} \quad (4)$$

where k_{tot} is the total dissociation rate constant, $k_{isom} + k_{-Cl}$ here. Apparently, $k_{tot} = k_{isom}$ when $E \leq E_0(-Cl)$ and $k_{tot} \approx k_{-Cl}$ otherwise. The $P_\tau(E)$ calculated with $\tau = 23$ μs, assumed as the lifetime of the present metastable ions, is shown in Figure 6. The calculations with the PST- and RRKM- $k_{-Cl}(E)$ gave the same result. The calculated $P_\tau(E)$ can be considered as the internal energy distribution of the molecular ions undergoing the metastable dissociation ignoring the energy deposition function by electron ionization. The probability at higher than $E_0(-Cl)$ is zero, indicating that the metastable ions dissociate exclusively by loss of HCl in agreement with the present experimental observation. Since the residence time of the molecular ion in the EI ion source is a few microseconds,[31] almost all of the molecular ions of E higher than $E_0(-Cl)$ would dissociate in the ion source together with some of E lower than $E_0(-Cl)$. The latter, occurring by tunneling, would be detected as the $C_3H_6^{\bullet+}$ peak in the normal mass spectrum. Namely, the molecular ions of E lower than $E_0(-Cl)$ can dissociate in the ion source as well as in the second field-free region, detected in the normal mass spectrum and metastable MIKE spectrum, respectively

Then, why is not the HCl loss detected near the dissociation threshold of the molecular ion in the PEPICO and PI experiments even though dissociations occurring on a microsecond time scale can be observed with these techniques? Since the molecule investigated has a thermal energy, the energy selection is not performed perfectly upon photoionization. Instead of a singly energy-selected ion, molecular ions having an energy distribution contribute to signals at a selected wavelength. Therefore, near the threshold it would be hard to select only the molecular ions having internal energies lower than $E_0(-Cl)$. When the molecular ions having an energy distribution near $E_0(-Cl)$ generated by a photon dissociated, the HCl loss would be covered by the much more abundant $Cl^\bullet$ loss. The low mass resolution of PEPICO technique can be another reason for no detection of the very weak $C_3H_6^{\bullet+}$ peak, of which m/z is less than the strong $C_3H_7^+$ peak by 1. If such an experiment is carried out at 0 K, the HCl loss will be observed exclusively below $E_0(-Cl)$ as in the present metastable dissociation.

The KERD shown in Figure 1b consists of two components. The abundance of the small-KER component is ~3%, estimated roughly from the probability at 0−10 kJ mol^{-1} KER. We do not understand its origin at the moment. Apparently the large-KER component is due to the dissociation to $CH_3CHCH_2^{\bullet+}$ + HCl. The maximum KER is ~60 kJ mol^{-1}. If the metastable dissociation occurs just below $E_0(-Cl)$, the available energy for the dissociation is estimated by MP2 calculations as ~50 kJ mol^{-1}, agreeing with the experimental one considering limited accuracy of theoretical calculations. The broad shape of the KERD, of which maximum probability is at the large KER not near the zero KER, is a characteristic of dissociation with a substantial reverse barrier, not determined statistically.[15,32] In the HCl loss, the first step, the isomerization by tunneling, occurs with a considerable reverse barrier, while the followed dissociation without. Since it is predicted that the final dissociation occurs within a picosecond, the intramolecular vibrational redistribution may not be effective after formation of the ion−molecule complex. Then, the dissociation step would not contribute to the KER effectively. A more rigorous dynamical study, such as those employing the classical trajectory method, would be needed to predict the KERD.

It is worthwhile to predict the dissociation of perdeuterated isopropyl chloride cation ($CD_3CDClCD_3^{\bullet+}$), even though it has not been investigated experimentally here. The critical energies for the isomerization (i.e., the DCl loss) and the $Cl^\bullet$ loss from this isotopomer, calculated at the MP2/6-311++G(d,p) level, are 60.82 and 36.77 kJ mol^{-1}, respectively. RRKM rate calculations were carried out with the same way as above (see Table 2 for the parameters used). The calculated rate constant for the $Cl^\bullet$ loss at 0.1 kJ mol^{-1} above its threshold is 9×10^7 s^{-1}. At the same energy, that for the DCl loss by tunneling is 2×10^1 s^{-1}. It is expected that the DCl loss that can occur by tunneling below the threshold of the $Cl^\bullet$ loss is too slow to be detected on a microsecond time scale. As a result, we predict that the DCl loss will be hardly detected in the metastable dissociation of perdeuterated isopropyl chloride cation.

4. Conclusions

Loss of HCl was observed in the metastable dissociation of isopropyl chloride cation, which was not detected in the previous experiments with energy-selected ions by photon. The observation could be interpreted by invoking quantum mechanical tunneling. The relative energies of the molecular ion and products obtained by MP2/6-311++G(d,p) calculations agree with experimental ones within about ±10 kJ mol^{-1}. According to the PES obtained by ab initio calculations, the HCl loss hardly occurs without considering tunneling. The tunneling-corrected RRKM model calculations showed that the metastable dissociation would occur by tunneling through an isomerization barrier to an ion−dipole complex below the threshold for the $Cl^\bullet$ loss. The available energy for the metastable dissociation from the measured KERD agrees with the predicted one from the ab initio and RRKM calculations within the accuracy of the calculations. Since it is predicted that the $Cl^\bullet$ loss occurs on a nanosecond time scale even just above the threshold, almost all of the molecular ions having internal energies higher than the threshold would dissociate fast in the ion source. The remaining molecular ions with lower energies would contribute to the HCl loss by tunneling in metastable dissociation. This work shows that the ability of tandem mass spectrometry to select metastable ions having lifetime of tens of microseconds is very useful to find a dissociation occurring by tunneling.

Acknowledgment. This work was supported by the Korea Research Foundation Grant (KRF-2004-041-C00169). The author thanks Professor Myung Soo Kim (Seoul National University) for use of the mass spectrometer and the Computer Center of Seoul National University for use of an IBM SP Nighthawk-2 computer.

References and Notes

(1) Heinrich, N.; Louage, F.; Lifshitz, C.; Schwarz, H. *J. Am. Chem. Soc*. **1988**, *110*, 8183.

(2) Polik, W. F.; Guyer, D. R.; Miller, W. H.; Moore, C. B. *J. Chem. Phys*. **1990**, *92*, 3471.

(3) Booze, J. A.; Weizel, K.-M.; Baer, T. *J. Chem. Phys*. **1991**, *94*, 3649.

(4) Keister, J. W.; Baer, T.; Thissen, R.; Alcaraz, C.; Dutuit, O.; Audier, H.; Troude, V. *J. Phys. Chem. A* **1998**, *102*, 1090.

(5) Hristendahl, G.; Uggerud, E. *Org. Mass Spectrom*. **1991**, *26*, 67.

(6) Kim, D. Y.; Choe, J. C.; Kim, M. S. *J. Phys. Chem. A* **1999**, *103*, 4602.

(7) Won, D. S.; Choe, J. C.; Kim, M. S. *Rapid Commun. Mass Spectrom*. **2000**, *14*, 1110.

(8) Miller, W. H. *J. Am. Chem. Soc*. **1979**, *101*, 6810.

(9) Baer, T.; Song, Y.; Ng, C. Y.; Liu, J.; Chen, W. *J. Phys. Chem. A* **2000**, *104*, 1959.

(10) Hudson, C. E.; Traeger, J. C.; Griffin, L. L.; McAdoo, D. J. *J. Phys. Chem. A* **2003**, *107*, 512.

(11) NIST Standard Reference Database 69, June 2005, *NIST Chemistry WebBook*.

(12) Baldwin, M.; Maccoll, A.; Miller, S. I. *Adv. Mass Spectrom*. **1966**, *3*, 259.

(13) Maccol, A.; Mathur, D. *Org. Mass Spectrom*. **1980**, *15*, 483.

(14) Cooks, R. G.; Beynon, J. H.; Caprioli, R. M.; Lester, G. R. *Metastable Ions*; Elsevier: Amsterdam, 1973.

(15) Baer, T.; Hase, W. L. *Unimolecular Reaction Dynamics: Theory and Experiments*; Oxford: New York, 1996.

(16) Chesnavich, W. J.; Bowers, M. T. In *Gas-phase Ion Chemistry*; Bowers, M. T., Ed.; Academic Press: New York, 1979; Vol. 1, pp 119−151.

(17) Frisch, M. J.; Trucks, G. W.; Schlegel, H. B.; Scuseria, G. E.; Robb, M. A.; Cheeseman, J. R.; Zakrzewski, V. G.; Montgomery, J. A., Jr.; Stratmann, R. E.; Burant, J. C.; Dapprich, S.; Millam, J. M.; Daniels, A. D.; Kudin, K. N.; Strain, M. C.; Farkas, O.; Tomasi, J.; Barone, V.; Cossi, M.; Cammi, R.; Mennucci, B.; Pomelli, C.; Adamo, C.; Clifford, S.; Ochterski, J.; Petersson, G. A.; Ayala, P. Y.; Cui, Q.; Morokuma, K.; Rega, N.; Salvador, P.; Dannenberg, J. J.; Malick, D. K.; Rabuck, A. D.; Raghavachari, K.; Foresman, J. B.; Cioslowski, J.; Ortiz, J. V.; Baboul, A. G.; Stefanov, B. B.; Liu, G.; Liashenko, A.; Piskorz, P.; Komaromi, I.; Gomperts, R.; Martin, R. L.; Fox, D. J.; Keith, T.; Al-Laham, M. A.; Peng, C. Y.; Nanayakkara, A.; Challacombe, M.; Gill, P. M. W.; Johnson, B.; Chen, W.; Wong, M. W.; Andres, J. L.; Gonzalez, C.; Head-Gordon, M.; Replogle, E. S.; Pople, J. A. *Gaussian 98, revision A.11.3*; Gaussian, Inc.: Pittsburgh, PA, 2002.

(18) Barrett, R. J. *Annu. Rev. Phys. Chem*. **1981**, *32*, 359.

(19) Scott, A. P.; Radom, L. *J. Phys. Chem*. **1996**, *100*, 16502.

(20) Pople, J. A.; Head-Gordon, M.; Raghavachari, K. *J. Chem. Phys.* **1987**, *87*, 5968.

(21) Eckart, C. *Phys. Rev.* **1930**, *35*, 1303.

(22) Beyer, T.; Swinehart, D. R. *ACM Commun.* **1973**, *16*, 379.

(23) Chesnavich, W. J.; Bowers, M. T. *J. Chem. Phys*. **1977**, *66*, 2306.

(24) Chesnavich, W. J.; Bowers, M. T. *J. Am. Chem. Soc.* **1977**, *99*, 1705.

(25) Yeh, I. C.; Kim, M. S. *Rapid Commun. Mass Spectrom.* **1992**, *6*, 115; 293.

(26) Lias, S. G.; Bartmess, J. E.; Liebman, J. F.; Holmes, J. L.; Levine, R. D.; Mallard, W. G. *J. Phys. Chem. Ref. Data* **1988**, *17* (Suppl. No. 1).

(27) Choe, J. C. *Int. J. Mass Spectrom*. **2005**, *245*, 53.

(28) *Handbook of Chemistry and Physics*, 76th ed.; Lide, D. R.; Ed.; CRC: Cleveland, OH, 1995.

(29) Lifshitz, C. *Mass Spectrom. Rev*. **1982**, *1*, 309.

(30) Lifshitz, C. *Adv. Mass Spectrom.* **1989**, *11*, 713.

(31) Burgers, P. C.; Holmes, L. J. *Int. J. Mass Spectrom. Ion Processes* **1984**, *58*, 15.

(32) Uggerud, E. *Mass Spectrom. Rev.* **1999**, *18*, 285.